Oncogene (2003) 22, 246–255

www.nature.com/onc

Ras-mediated apoptosis of PC CL 3 rat thyroid cells induced by RET/PTC oncogenes

Maria Domenica Castellone[1], Anna Maria Cirafici[1], Gabriella De Vita[1], Valentina De Falco[1], Luca Malorni[1], Giovanni Tallini[2], James A. Fagin[3], Alfredo Fusco[1], Rosa Marina Melillo[1] and Massimo Santoro*[,1]

[1]*Istituto di Endocrinologia ed Oncologia Sperimentale del CNR, c/o Dipartimento di Biologia e Patologia Cellulare e Molecolare, University 'Federico II', Naples, Italy;* [2]*Department of Pathology, University of Yale, USA;* [3]*Division of Endocrinology, University of Cincinnati College of Medicine, Ohio 45267-0547, USA*

RET gene rearrangements, which generate chimeric RET/PTC oncogenes, are early events in the evolution of thyroid papillary carcinomas. Expression of RET/PTC oncogenes promotes neoplastic transformation of cultured thyroid cells and of thyroid glands in transgenic mice. Notwithstanding these oncogenic effects, we have found that the expression of two RET/PTC oncogenes (H4-RET and RFG-RET) induces apoptosis of rat thyroid PC CL 3 cells. Promotion of thyroid cell death depends on the kinase activity of RET/PTC and on the phosphorylation of a tyrosine residue (tyrosine 1062) that maps in the carboxy-terminus of the RET protein. Tyrosine 1062 is essential for RET/PTC-mediated activation of the Ras/ERK pathway. Inhibition of Ras/ERK by a dominant negative Ras or by the MEKI inhibitor, PD98059, obstructed RET/PTC-mediated apoptosis. We also show that signals transmitted by tyrosine 1062 mediate proapoptotic events like Bcl-2 down regulation and Bax upregulation, and that adoptive overexpression of Bcl-2 overcomes RET/PTC-induced apoptosis. Thus, gene rearrangements that generate RET/PTC oncogenes subvert RET function by converting it into a chronically active kinase that is constitutively phosphorylated on tyrosine 1062. In turn, Y1062 phosphorylation transmits not only mitogenic but also proapoptotic signals to thyroid cells.

Oncogene (2003) **22,** 246–255. doi:10.1038/sj.onc.1206112

Keywords: Kinase; Carcinoma; Survival; Ras; Tyrosine; Thyroid; Oncogene; TUNEL

Introduction

Papillary carcinomas (PTC) are the most prevalent malignancies of the thyroid gland. In PTC, chromosomal inversions or translocations cause the recombination of the intracellular kinase-encoding domain of the RET receptor to heterologous genes, generating chimeric oncogenes designated RET/PTC (Jhiang, 2000; Pierotti, 2001). RET/PTC1, the H4-RET fusion (Grieco *et al.,* 1990), and RET/PTC3, the RFG-RET fusion (Santoro *et al.,* 1994a), are the most prevalent variants. RET/PTC oncogenes are able to initiate thyroid carcinogenesis as shown by the fact that RET/PTC-transgenic mice develop papillary thyroid carcinomas (Jhiang, 2000). The observation that not all RET/PTC-transgenics develop carcinomas suggests that secondary stochastic events are required for malignant progression. RET/PTC oncogenes are highly prevalent in clinically silent small papillary carcinomas (microcarcinomas) and in very small thyroid lesions with uncertain malignant potential, suggesting that they are early events in tumorigenesis and are not sufficient for the development of symptomatic thyroid cancers (Viglietto *et al.,* 1995; Sugg *et al.,* 1998; Corvi *et al.,* 2001).

In RET/PTC oncoproteins, the fusion with partners possessing protein-protein interaction motifs provides the RET kinase with a dimerizing interface. This results in constitutive dimerization and phosphorylation of the chimeric oncoproteins and in constant upregulation of RET signaling (Tong *et al.,* 1997; Monaco *et al.,* 2001). RET signaling depends on tyrosine 1062, an autophosphorylation site positioned in its carboxy-terminal tail and, thus, retained in the RET/PTC oncoproteins. *p*Y1062 is embedded in an NKL*p*Y (single-letter amino-acid code) motif and mediates recruitment of various proteins (for a review see Manie *et al*., 2001) and references therein. Among them, Shc and FRS2 are recruited to RET *p*Y1062 via their phosphotyrosine binding (PTB) domains (Mercalli *et al*., 2001; Melillo *et al.,* 2001); by bridging RET-to-Grb2-Sos complexes, Shc and FRS2 play a key role in the activation of Ras small GTPases.

The effect of oncogenes in thyrocytes can be studied in various culture systems, including rat thyroid cell lines and primary cultures of rat, dog, sheep, and human

*Correspondence: M Santoro, Istituto di Endocrinologia ed Oncologia Sperimentale del CNR, Università di Napoli 'Federico II', via S. Pansini 5, 80131 Naples, Italy;
E-mail: masantor@unina.it
Received 14 June 2002; revised 2 October 2002; accepted 4 October 2002

thyroid. The different characteristics of these model cell systems have been recently reviewed (Kimura *et al.,* 2001). Although results obtained with cultured cells must be cautiously extrapolated to *in vivo* models, these different cell systems have been proven useful to study differentiation, survival, and growth regulation in an epithelial thyroid cell setting. PC CL 3, a continuous line of Fischer rat thyroid cells, constitutes one of the available thyrocyte models. PC CL 3 cells express differentiation markers and depend on a mixture of 6 hormones, including TSH and insulin, for proliferation (Fusco *et al.,* 1987a). We have previously shown that the expression of the RET/PTC1 oncogene causes hormone-independent proliferation and abolishes differentiated gene expression of PC CL 3 cells (Santoro *et al.,* 1993). These data were in agreement with resistance to thyrotropin induced by other tyrosine kinases, such as the EGFR (Roger and Dumont, 1982) and the HGFR (Dremier *et al.,* 1994), in primary dog thyroid cells. Here we show that, in addition to these mitogenic and de-differentiative effects, the RET/PTC1 and RET/PTC3 oncogenes induce apoptosis of PC CL 3 cells, and that this effect is dependent on RET/PTC enzymatic activity and *p*Y1062-mediated triggering of the Ras signaling cascade, a process that in turn leads to an increased Bax to Bcl-2 ratio.

Results

RET/PTC1 and RET/PTC3 induce apoptosis of PC CL 3 cells

We cloned RET/PTC1 and RET/PTC3 cDNAs (Figure 1a) into a mammalian expression vector (pcDNA3) resistant to neomycin. PC CL 3 cells were transfected with RET/PTC I and RET/PTC3 as well as with the empty vector and selected for 2 weeks in neomycin containing medium. PC CL 3 cells transfected with the empty vector produced many large colonies, whereas RET/PTC I and three transfection resulted in a few small colonies (Figure 1b). The number of colonies formed by RET/PTC-transfected cells was approximately ten times smaller with respect to colonies formed by empty-vector-transfected cells (see also Figure 3). To determine whether this reflected the cytotoxic effects of RET/PTC constructs due to apoptosis, neomycin-resistant PC CL 3 colonies transfected with RET/PTC oncogenes or with the empty vector were pooled and expanded. Single clones were also isolated (three for each construct). The results obtained with isolated clones were identical to those obtained with mass population. Thus, results described thereafter are those obtained with mass populations. The expression of the

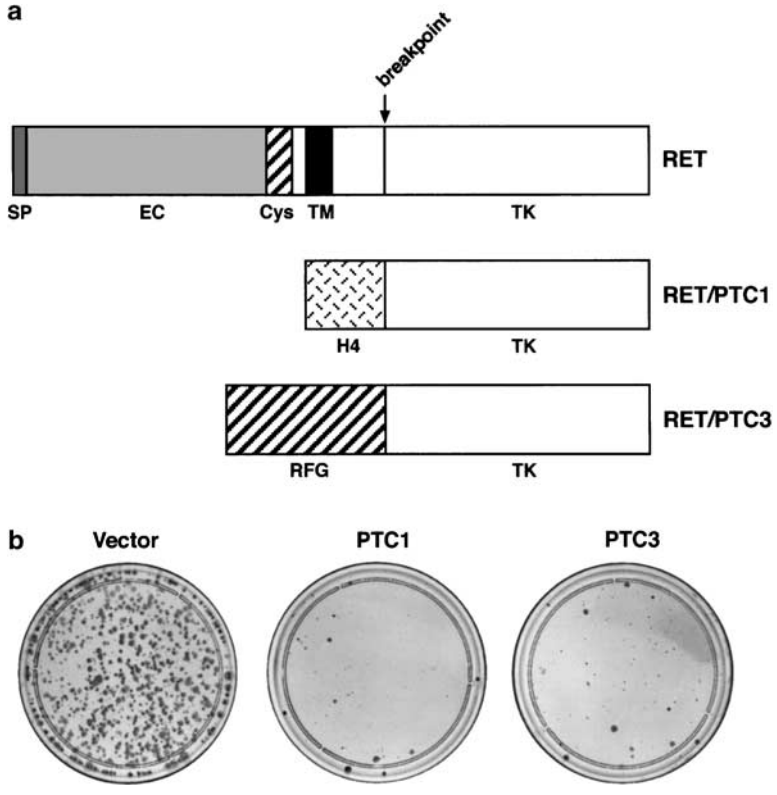

Figure 1 (**a**) Schematic representation of the constructs used in this study: SP, signal peptide; EC, extracellular domain; Cys, cysteine-rich domain; TM, transmembrane; TK: tyrosine kinase. The RET/PTC breakpoint is indicated. (**b**) PC CL 3 cells were transfected with RET/PTC1, RET/PTC3 or the empty vector and selected in neomycin-containing medium. Two weeks later, cells were stained with crystal violet and photographed. A representative experiment of at least three independent assays is shown

two oncoproteins was verified by Western blot with anti-RET antibodies (Figure 2a). As shown by the growth curves reported in Figure 2b, RET/PTC-transfected cells proliferated in complete medium more slowly than vector-transfected cells. Since the net rate of growth of a cell population results from the difference between proliferation and cell death, these findings could indicate that RET/PTC oncogenes induce thyrocyte apoptosis. Thus, flow cytometry was used to measure the percentage of apoptotic cells. Vector-, RET/PTC 1 and RET/PTC3 -transfected cells were plated overnight. Floating and adherent cells were collected 72 h later, fixed, stained with propidium iodine and processed for flow cytometry. The frequency of cells with hypodiploid DNA content was significantly higher among RET/PTC 1 and RET/PTC3 cells (25 ± 3 and $20 \pm 3\%$) than among vector-transfected cells ($5 \pm 2\%$) (Figure 2c). Finally, internucleosomal DNA fragmentation was evaluated by the TUNEL assay in RET/PTC 1 and RET/PTC3-expressing cells. As a positive control, we used a potent apoptotic stimulus (2 ng/ml vincristme) (data not shown). Apoptosis was measured in five randomly selected microscopic fields. One representative microscopic field is reported in Figure 2d. Apoptotic nuclei were rare ($<5\%$) in vector-transfected cells. Approximately, 20% of the nuclei of RET/PTC-oncogene-expressing cells were apoptotic. Taken together, these results indicate that RET/PTC-oncogene-expressing PC CL 3 cells are more prone to perish by apoptosis than vector-transfected cells.

Tyrosine Y1062 mediates RET/PTC apoptotic effects

In addition to the autocatalytic tyrosine Y905 that is implicated in enzymatic function, full-length RET has five major phosphoiylation sites (Y687, Y826, Y1015,

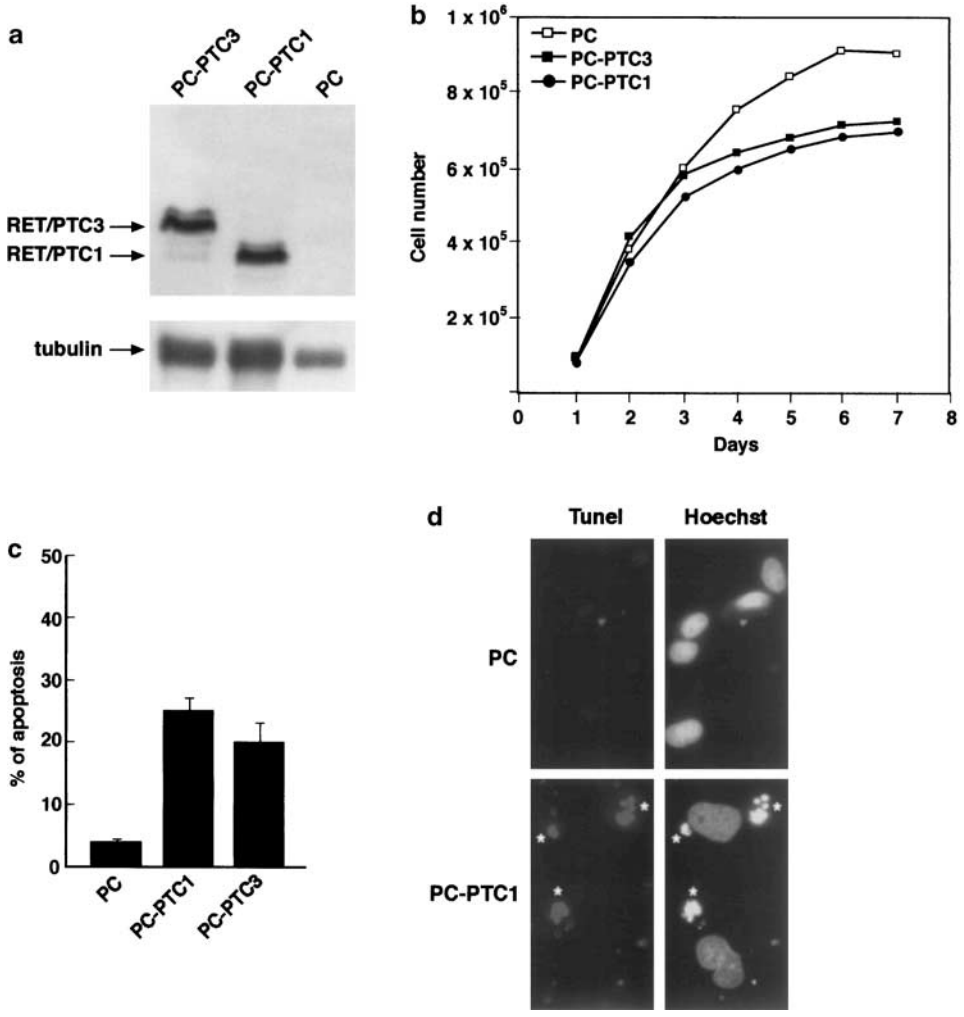

Figure 2 (**a**) Protein lysates (100 µg) underwent Western blotting with anti-RET specific antibody. Immunocomplexes were revealed by enhanced chemiluminescence. Anti-α-tubulin antibodies were used for normalization. (**b**) A total 50000 cells were plated and counted daily starting 1 day after plating. Data are the means of three experiments. (**c**) The indicated cell types were subjected to flow cytometry 72 h after plating. The percentage of cells in the subG1 compartment is indicated. Bars are the mean ± s.d. of three independent experiments made in duplicate. (**d**) The TUNEL reaction was performed on the indicated cell lines. Cells were photographed under an epifluorescent microscope to detect TUNEL-positive cells (TMR-dUTP, red) and total cells on the glass slide (Hoechst, blue stain): representative microscopic fields are shown. Apoptotic cells are marked with asterisks

Y1029, and Y1062) (Liu *et al.,* 1996). Because of the truncation, rearranged RET/PTC proteins maintain only four of these tyrosines and lack Y687. Phosphorylated Y1015 (*p*Y1015) interacts with phospholipase Cγ (PLCγ) (Borrello *et al.,* 1996), whereas *p*Y1062 is a docking site for the recruitment of multiple effectors (see Introduction). We constructed a panel of mutants in the RET/PTC1 background. These included a kinase-inactive RET/PTC1 (RET/PTC1 K-), carrying the substitution of the catalytic lysine (K758) to methionine, a RET/PTC1 mutant (RET/PTCI 4F) in which the four major autophosphorylation sites (Y826, Y1015, Y1029, and Y1062) were substituted by phenylalanines, and single mutants in Y1015 (Y10I5F) or Y1062 (Y10623F) (Figure 3a). Each construct was transfected into HEK293 cells and analyzed with the aid of SDS gels and anti-RET antibodies: each transfection produced proteins of the appropriate mobility (not shown). PC CL 3 cells were transfected in triplicate with these constructs or the empty vector and selected in neomycin-containing medium for 2 weeks. Colonies were counted after the selection and the results are summarized in the bar-graphs of Figure 3b. Differently from wild-type RET/PTC1, the cytotoxic effects of the kinase-inactive mutant were barely detectable. RET/PTC-cytotoxicity depended on the integrity of the major phosphorylation sites because the 4F mutant lacked cytotoxic effects; in particular, Y1062, but not Y1015, was essential for cytotoxicity.

To verify whether apoptosis was directly because of RET/PTC signaling rather than being a secondary and late effect of thyroid cell transformation, we set up a transient assay in which cells were analyzed 60 h after transfection. RET/PTC1 and its kinase-inactive and Y1062F mutants, were transiently expressed in PC CL 3 cells together with trace amounts of EGFP to track transfected cells. Internucleosomal DNA fragmentation was evaluated by the TUNEL assay. Apoptosis was measured in five randomly selected microscopic fields; at least 100 EGFP-positive cells were counted. One representative microscopic field and the average results of three experiments are reported in Figure 4. Apoptotic nuclei were rare (<5%) in vector-transfected cells. RET/PTC1 induced massive apoptosis. RET/PTC-mediated apoptosis depended on its enzymatic activity and on phosphorylation of Y1062. In fact, the apoptotic rates of cells transfected with the kinase-dead and Y 1062F mutants were significantly lower than that induced by the wild-type construct. Still, the Y1062F mutant induced a modest apoptotic rate indicating that other signalling residues may contribute to RET/PTC-induced cell suicide (Figure 4).

Apoptosis of PC CL 3 cells is mediated by RET/PTC-dependent up regulation of the Ras/ERK signaling pathway

Ras activation is promoted by the coupling of phosphorylated Y1062 of RET with Grb2-Sos complexes via multiple docking proteins (for a review see Manie *et al*. (2001) and references therein). A key cellular response to Ras is transduced through the extracellular

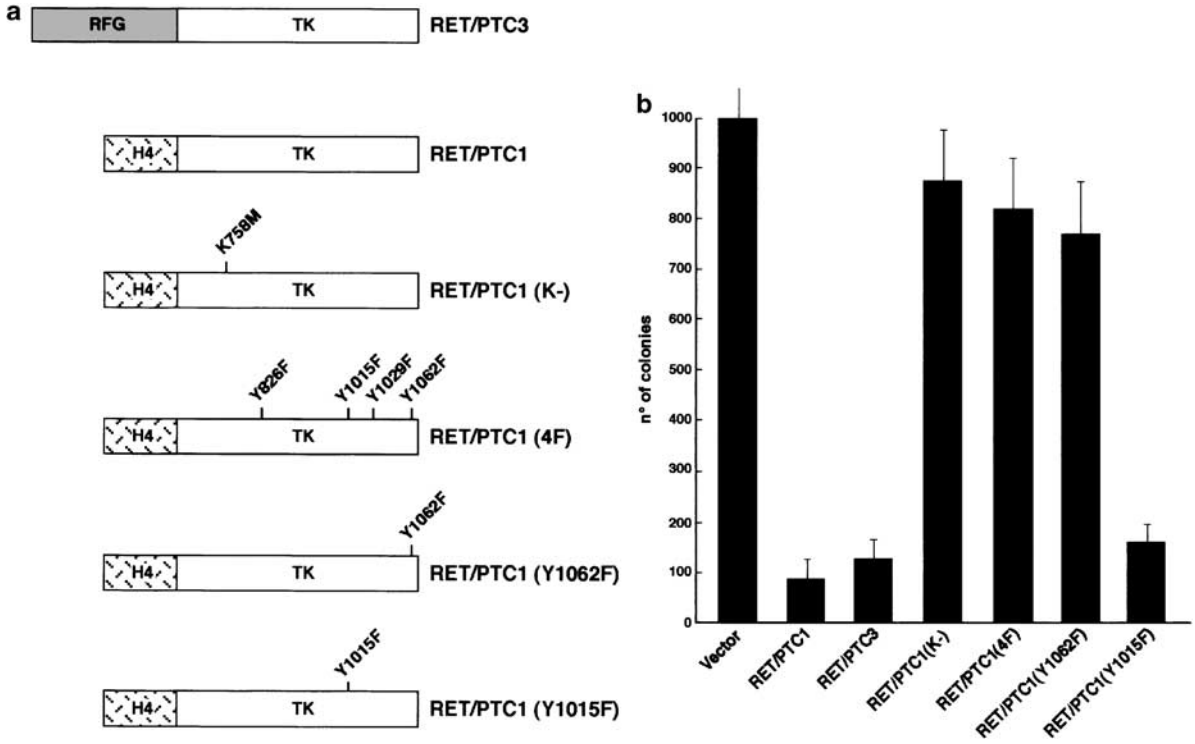

Figure 3 (**a**) Schematic representation of the RET/PTC constructs used in this study. (**b**) PC CL 3 cells were transfected with the indicated constructs and selected in neomycin-containing medium. Two weeks later cells were stained with crystal violet and counted. Bars are the mean±s.d. of three independent experiments made in duplicate

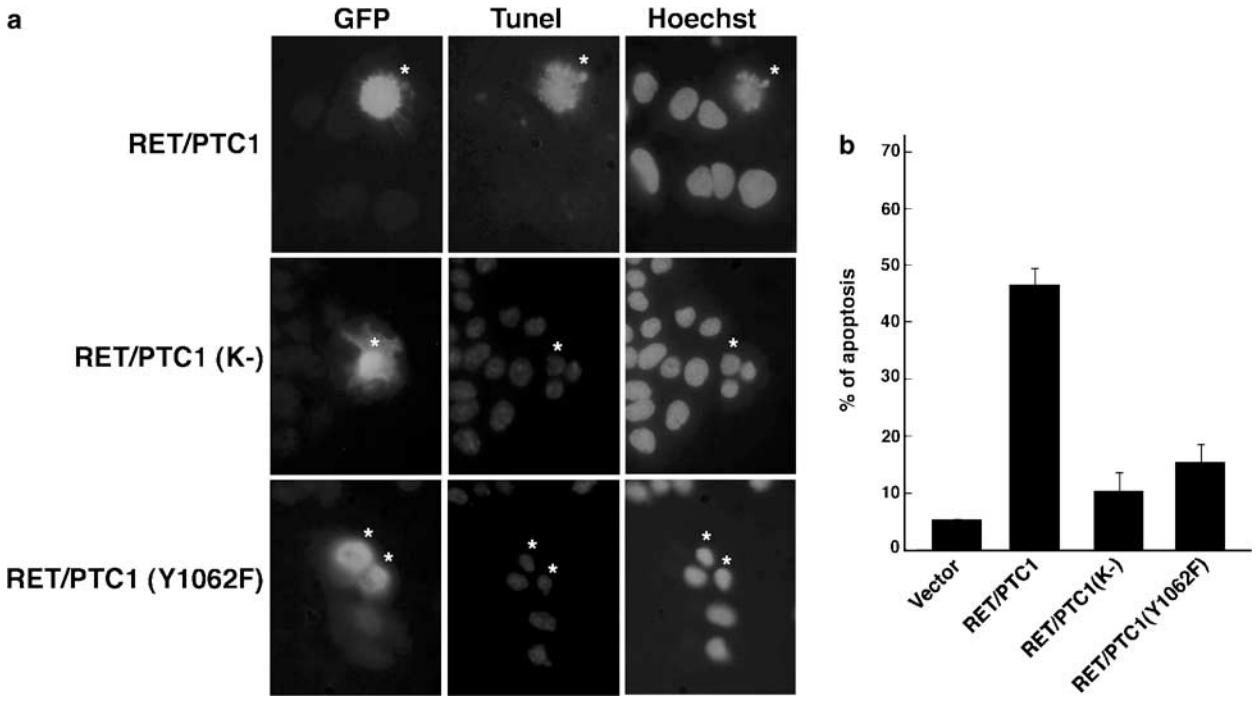

Figure 4 The indicated constructs were transiently expressed in PC CL 3 cells together with EGFP, and 60 h later the TUNEL reaction was performed. Cells were photographed under an epifluorescent microscope to detect transfected cells (EGFP, green), TUNEL-positive cells (TMR-dUTP, red) and total cells on the glass slide (Hoechst, blue stain). (**a**) Representative microscopic fields: apoptotic cells are marked with asterisks. (**b**) Bars are the mean ± s.d. of three assays. Apoptotic cells were calculated by counting at least 100 EGFP-positive cells in five randomly selected microscopic fields

ligand-regulated kinase (ERK) pathway resulting from the sequential activation of Raf, MEK and the p42 and p44 ERK. A pull-down assay showed that PC-RET/PTC1 cells constitutively activate Ras (Figure 5a); robust activation of ERK was shown by *in vitro* kinase assay (Figure 5b) and immunoblot with phosphospecific antibodies (Figure 5c). As expected, Ras/ERK activation depended on Y1062 (Figure 5a,b). We found that 35 μM was the minimal concentration of PD98059 (a selective MEK1 inhibitor) that blocked ERK activation in PC-RET/PTC 1 cells (Figure 5c). Stable expression of activated (V12) H-Ras in PC CL 3 cells induces a phosphorylation of MAPK more intense than that induced by RET/PTC1 (Figure 5d).

While Ras/ERK activation protects neuronal cells from apoptosis (Xia *et al.,* 1995), strong activation of this pathway has proapoptotic effects in other cell types (Kauffmann-Zeh *et al*., 1997). Thus, we sought to determine whether Ras/ERK activation by RET/PTC Y1062 was essential for RET/PTC-mediated apoptosis. RET/PTC1 was transiently expressed in PC CL 3 cells together with trace amounts of EGFP with and without a five-fold excess of the dominant-interfering RasN17 mutant. At 48 h after transfection, cells not receiving RasN17 were treated with PD98059 (35 μm) or vehicle for an additional 12 h, and the apoptotic rate was evaluated by the TUNEL assay. RasN17 expression and treatment with PD98059 significantly reduced RET/PTC1-induced apoptosis (Figure 5e). Both treatments did not completely abrogate RET/PTC-mediated apoptosis. However, their effects were specific as we did not observe any protective effect exerted by RasN17 and by PD98059 on cell death induced by an apoptotic trigger other than RET/PTC (100 nglmt vincristine for 12 h) (Figure 5f). Finally, in agreement with the toxic effects exerted by the Ras pathway in PC CL 3 cells, expression of constitutively active H-Ras (V12) had potent proapoptotic effects (Figure 5e).

RET/PTC tyrosine 1062 mediates Bcl-2 down regulation and Bax up regulation in PC-RET/PTC cells

Bcl-2 family proteins have emerged as fundamental regulators of the discharge of cytochrome C from mitochondria and, in turn, apoptosome formation during apoptosis. Bcl-2, Bcl-x_L and Mcl-l are anti apoptotic proteins, and Bax, Bak, Bok and 'BH3-domain only' are proapoptotic proteins (Evan and Littlewood, 1998). Activated proapoptotic Bax and Bak promote mitochondria permeabilization by forming a multimeric pore causing the initial efflux of cytochrome *c*. Antiapoptotic Bc1-2 proteins obstruct this process by sequestering 'BH3-domain only' molecules; thus preventing the allosteric activation of Bax. The ratio between antiapoptotic and pro-apoptotic Bcl-2 proteins ultimately determines cell susceptibility to apoptotic death (Evan and Littlewood, 1998).

To gain insight into RET/PTC-mediated apoptosis, we investigated the expression levels of Bcl-2, Bcl-x_L,

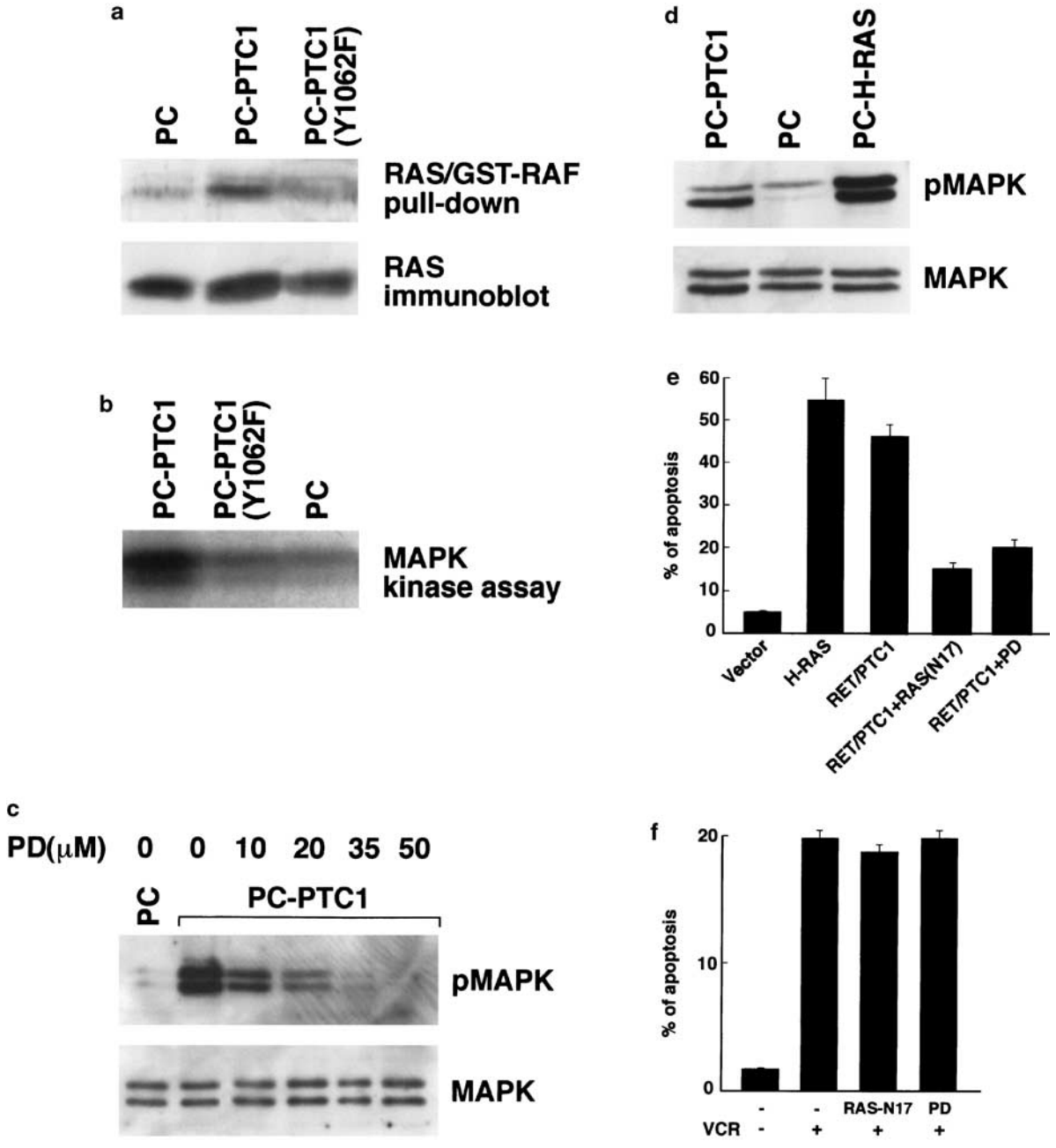

Figure 5 (**a**) Affinity precipitation of Ras-GTP from protein lysates with agarose immobilized Raf1 RBD and detection by blot with a pan-isoform specific anti-Ras. A total of 100 μg of proteins were immunoblotted with anti-panRas for normalization. (**b**) ERK were immunoprecipitated from protein lysates. The immunoprecipitates were incubated with MBP and labeled ATP; the reaction product was analyzed by SDS–PAGE followed by autoradiography. (**c**) RET/PTC1-expressing PC CL 3 cells were treated for 12 h with the indicated amounts of PD98059 or vehicle (−). Proteins were extracted and immunoblotted with antibodies specific for ERK or phosphorylated ERK. (**d**) Proteins were extracted from the indicated cell lines and immunoblotted with antibodies specific for ERK or phosphorylated ERK. (**e**) The indicated constructs were transiently expressed in PC CL 3 cells together with EGFP, and 60 h later the TUNEL reaction was performed. Where indicated, cells were treated with PD98059 (35 μM) 12 h before harvesting. Cells were photographed and Percentage of apoptosis reported as described in the legend to Figure 4. (**f**) RasN17 was transiently expressed in PC CL 3 cells together with EGFP, and 60 h later the TUNEL reaction was performed. Where indicated, cells were treated with PD98059 (35 μM) or vincristine (100 ng/ml) 12 h before harvesting

Bad and Bax by immunoblot. PC CL 3 cells expressing RET/PTC1 had significantly increased levels of Bax and reduced levels of Bcl-2 (Figure 6). BCI-x_L and Bad levels remained essentially unchanged (not shown). The changes in Bax and Bcl-2 depended on the integrity of Y1062; indeed, cells expressing the Y1062F mutant showed wild type levels of both proteins. Intriguingly, also v-Ha-Ras-expressing cells had increased Bax and

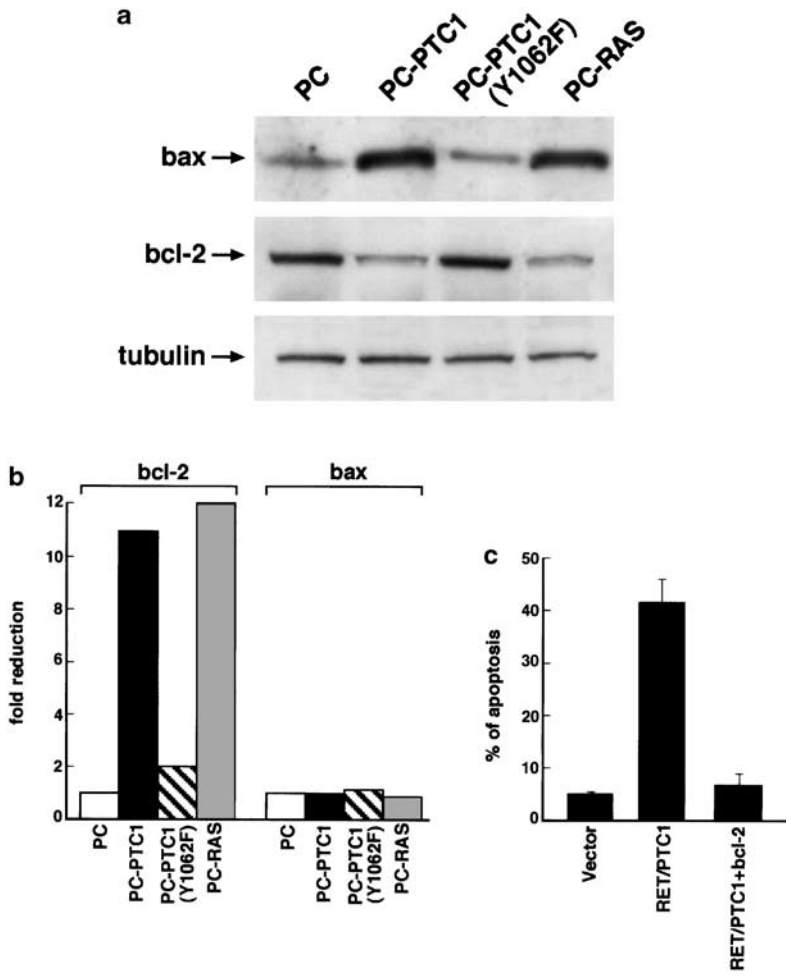

Figure 6 (**a**) Protein lysates (100 μg) underwent Western blotting with the indicated antibodies. Immunocomplexes were revealed by enhanced chemiluminescence. Anti-α-tubulin antibodies were used for normalization. (**b**) Quantitative real-time PCR was used to calculate Bcl-2 and Bax mRNA fold changes in the indicated cell lines. Results are the average of three independent amplifications. (**c**) The indicated constructs were transiently expressed in PC CL 3 cells together with EGFP, and 60 h later the TUNEL reaction was performed. Bars are the mean ± s.d. of three assays

decreased Bcl-2 levels, supporting the possibility that these proapoptotic expression changes are mediated by Ras (Figure 6a). We performed real-time RT-PCR amplification to verify whether Bcl-.2 and Bax modulation occurred at mRNA level. Bcl-2 mRNA down regulation (>10 fold) was readily detected in RET/PTC1- and v-Ha-Ras expressing cells, but not in cells expressing the Y1062F RET/PTC mutant. In the case of Bcl-2, changes were lower at mRNA level than at protein level. Bax mRNA levels were unchanged in transformed cells, pointing to a post-transcriptional level of regulation (Figure 6b).

To verify whether changes in the ratio of Bax to Bcl-2 proteins are a factor in the apoptosis of PC-RET/PTC cells, RET/PTC1 was transiently expressed in PC CL 3 cells with or without a three-fold excess of a Bcl-2 expression vector; transfected cells were tracked with trace amounts of EGFP. Apoptosis was evaluated by the TUNEL assay. Bcl-2 expression prevented RET/PTC1-induced apoptosis (Figure 6c).

Discussion

Here we show that the expression of RET/PTC oncogenes causes apoptosis of rat thyroid epithelial cells. Transient expression of RET/PTC induces apoptosis of a large fraction (~50%) of transfected PC CL 3 cells, whereas a lower fraction (~25%) undergo suicide upon stable expression of RET/PTC. These findings are consistent with a model in which acute RET/PTC signaling has proapoptotic effects; cells chronically exposed to RET/PTC signaling *in vitro* eventually undergo secondary changes that inactivate the apoptotic cascade and partially mitigate the apoptotic effects of RET/PTC.

RET/PTC-mediated apoptosis depends on RET/PTC's enzymatic activity and on the phosphorylation of the tyrosine residue corresponding to Y1062 in full-length RET. Intriguingly, in thyroid cells, tyrosine 1062 also mediates the loss of the differentiation markers and the ability to proliferate in the absence of six hormones

(Melillo R M, Cirafici A M, Castellone M D, Malorni L and Santoro M, in preparation). Thus, signals originating from a single tyrosine cause autonomous proliferation and de-differentiation of thyrocytes and are detrimental to cell survival.

Activation of MAPK is a downstream event common to the triggering of different tyrosine kinases in thyroid cells (Lamy *et al.,* 1993). Tyrosine 1062 mediates sustained Ras/ERK activation by RET/PTC (this paper and Melillo *et al.,* 2001). We show that Ras/ERK is an important component of RET/PTC apoptotic signaling; indeed, PD98059, used at the minimally effective concentration verified to block kinase activation, and expression of a dominant negative Ras prevented cell death. Ras can promote both cell death and cell survival, depending on cell type, the nature of concomitant regulatory signals, and the effectors used. At least in some systems, Ras triggers apoptosis by activating Raf/ERK (Downward, 1998). In addition to the data reported in the present paper, there is compelling evidence that Ras activation promotes apoptosis of thyroid cells. PC CL 3 thyroid cells undergo massive apoptosis consequent to acute activation of Ras and MEK 1 (Shirokawa *et al.,* 2000). H-Ras-mediated apoptosis was shown to depend on concomitant activation of cyclic AMP (Shirokawa *et al.,* 2000). Cheng (Cheng and Meinkoth, 2001) reported that constitutive expression of oncogenic H-Ras sensitizes Wistar rat thyroid cells to apoptosis induced by loss of anchorage. In this system, upon detachment (and thus when integrin signaling is impaired) cell survival rather than cell death was found to be dependent on sustained MAPK activation. Although dependent on Ras, RET/PTC-mediated apoptosis is not dependent on concomitant cAMP activation (Castellone MD, unpublished). Thus, although sustained Ras/ERK activation is in general proapoptotic for thyrocytes, it is likely that specific concomitant signals originating from various oncoproteins are able to modulate the cell's response to death-promoting effects in different growth conditions. Intriguingly, we have previously reported that coexpression of activated Ras promotes tumorigenesis of RET/PTC1-expressing PC CL 3 cells (Santoro *et al.,* 1993). However, consistent with a proapoptotic role exerted by Ras signalling, Ras expression did not reduce the apoptotic rate of PC CL 3-RET/PTC cells (data not shown). Thus, it appears that Ras signalling can play a dual role: it is both necessary for the establishment of the transformed phenotype, and is detrimental for survival of RET/PTC-transformed thyrocytes.

We show that in RET/PTC-expressing PC CL 3 cells, Ras-mediated signaling is involved in the up regulation of the proapoptotic Bax and in the down regulation of the antiapoptotic Bcl-2 protein. Interestingly, such changes are likely because of different mechanisms: Bcl-2 is significantly downregulated at mRNA level, whereas Bax is modified only at a post-transcriptional level.

Cancer results from derangement of the critical balance between the rate of cell division and programmed cell death. Apoptosis induced by deregulated oncogenes must be forestalled for a tumor to become established. Whereas thyroid cancer is relatively infrequent, occult microcarcinomas or minimal lesions with uncertain malignant potential are very frequent in random autopsy screenings (up to 35.6%) suggesting that as yet unknown factor(s) inhibit tumor progression. These clinically silent thyroid tumors are very often RET/PTC-positive (Viglietto *et al.,* 1995; Sugg *et al.,* 1998; Corvi *et al.,* 2001). Our findings suggest that at least one of the factors that could limit the expansion of small tumors sustaining RET gene rearrangements is the proapoptotic activity of RET/PTC. During tumor progression, secondary events can be selected to suppress RET/PTC apoptosis and to promote the expansion of the neoplastic clones. For instance, secondary genetic changes causing overexpression Bcl-2 or activation of other cell survival pathways as overexpression of Akt or downmodulation of PTEN, both events reported to occur in thyroid cancer (Gimm, 2001), can effectively contrast RET/PTC-proapoptotic effects in thyroid carcinomas.

Materials and methods

Plasmids and antibodies

All the RET constructs used in this study encode the short (RET-9) spliced form and were cloned in pCDNA3(Myc-His) (Invitrogen, Groningen, The Netherlands). RET/PTCI and RET/PTC3 constructs are described elsewhere (Melillo *et al.,* 2001). The point mutants were generated by site-directed mutagenesis using the QuickChange mutagenesis kit (Stratagene, La Jolla, CA, USA). The mutations were confirmed by DNA sequencing. RET/PTC1 (K-) is a kinase-dead mutant, carrying the substitution of the catalytic lysine (residue 758 in full-length RET) with a methionine. The RET/PTC1 mutant carrying the substitution to phenylalanine of four tyrosines (Y826, Y1015, Y1029 and Y1062) is referred to as RET/PTCI(4F). RET/PTC1(Y1015F) and RET/PTC1(Y1062F) are single mutants in residues 1015 or 1062. For simplicity, we number the residues of RET/PTC proteins according to the corresponding residues in unrearranged RET. The Bcl-2 expression vector (pBabe-Bcl-2) was a kind gift of R Maestro (Maestro *et al.,* 1999).

Polyclonal anti-RET antibodies were raised using the kinase domain of the protein (Santoro *et al.,* 1994b). Anti-phosphotyrosine antibodies (4G10) were from Upstate Biotechnology Inc. (Lake Placid, NY, USA). Rabbit polyclonal anti-MAPK (#9101) and antiphospho-MAPK (#9102) antibodies were from New England Biolabs (Beverley, MA, USA). Bcl 2 (N-19, sc-492) and Bax (P-19, sc-526) antibodies were from Santa Cruz Biotechnology (Santa Cruz, CA, USA). Monoclonal anti-α-tubulin was from Sigma Chemical Co. (St Louis, MO, USA). Secondary antibodies were from Santa Cruz Biotechnology

Cell culture and transfections

Parental and transformed PC CL 3 cells were cultured in Coon's-modified Ham F12 medium supplemented with 5% calf serum and a mixture of thyrotropin (10 mU/ml), hydrocortisone (10 nM), insulin (10 μg/ml), apo-transferrin (5 μg/ml), somatostatin (10nglml) and glycyl-histidyl-lysine (10 ng/ml) (Sigma Chemical Co.) according to Fusco *et al.* (1987b). For stable transfections, 5×10^5 cells were plated 48 h before transfection in 60-mm tissue culture dishes. The

medium was changed to Dulbecco's modified Eagle's medium (DMEM) (GIBCO) containing 5% calf serum and six hormones. After 3 h calcium phosphate DNA precipitates were incubated with the cells for 1 h. DNA precipitates were removed, and cells were washed with serum-free DMEM and incubated with 15% glycerol in *N*-2-hydroxyethylpiperazine-*N*′-2-ethanesulfonic acid (HEPES) - buffered saline for 2 mm. Finally, cells were washed with DMEM and incubated in Coon's modified F12 medium supplemented with 5% calf serum and the six hormones. For the colony formation assay, colonies were counted after 2 weeks of G418 (neomycin) selection. Transfected cells were fixed in 11% glutaraldehyde in PBS, rinsed in distilled water and stained with 0.1% crystal violet in 20% methanol for 15 min and photographed.

Flow cytometry

Cells were harvested when subconfluent, fixed in methanol for 1 h at −20°C, rehydrated in PBS for 1 h at 4°C, and then treated with RNase A (100 U/ml) for 30 min. Propidium iodide (25 mg/ml) was added to the cells, and samples were analyzed with a FACScan flow cytometer (Becton Dickinson, San Jose, CA, USA) interfaced with a Hewlett-Packard computer (Palo Alto, CA, USA).

TUNEL assay

Terminal desoxynucleotidyl transferase (TdT)-mediated desoxyuridine triphosphate (dUTP) nick end-labeling (TUNEL) was performed on stably or transiently transfected cells with the *in situ* Cell Death Detection Kit, from Roche Molecular Diagnostics (Basel, Switzerland) according to the manufacturer's instructions. For transient transfections, cells were transfected as indicated above. Transfected cells were identified with trace amounts (0.5 μg) of the plasmid encoding enhanced Green Fluorescent Protein (pEGFP, Clontech Laboratories, Palo Alto, CA, USA). After transfection (8 h later), an equal number (5×10^3) of cells from the different lines was seeded onto 24-well plates (Costar Corp., Corning Incorporated, NY, USA) containing 1.4 cm^2 glass coverslips. Cells were fixed in a freshly prepared solution of 2% (w/v) paraformaldehyde in PBS pH 7.4 for 60 min at room temperature and permeabilized by soaking the coverslips for 2 min on ice in Hepes–Triton X-100 buffer (20 mm Hepes pH 7.4, 300 mM sucrose, 50 mM NaC1, 3 mM $MgC1_2$ and 0.5% Triton X-100). Coverslips were rinsed twice with PBS, air-dried and subjected to the TUNEL reaction. All coverslips were counterstained in PBS containing Hoechst 33258 (final concentration, 1 μg/ml; Sigma Chemical Co.), rinsed in water and mounted in a 50% glycerol solution in PBS. The fluorescent signal, emitted by the red fluorescent tetramethyl rhodamine (TMR)-labeled dUTP incorporated into fragmented DNA, was visualized with an epifluorescent microscope (Axiovert 2, Zeiss) (equipped with a 100x lens) interfaced with the image analyzer software KS300 (Zeiss).

Protein studies

Protein extractions and Western blot were performed according to standard procedures. Protein concentration was estimated by a modified Bradford assay (Bio-Rad, Munich, Germany). Immune complexes were detected with the enhanced chemiluminescence kit (Amersham Pharmacia Biotech, Little Chalfort, UK). For the ERK immunocomplex kinase assay, protein lysates (500 μg) were incubated with 2 μl of the specific antibody for 1 h at 4°C, immunocomplexes were recovered with protein A-Sepharose (Amersham Pharmacia Biotech). Precipitates were washed six times in lysis buffer and incubated with 20 μg of myelin basic protein as a substrate. Intensifying screens were used for autoradiography. Signal intensity was analyzed at the Phosphorimager (Typhoon 8600, Amersham Pharmacia Biotech) interfaced with the ImageQuant software. Ras activation was measured by the Ras activation assay kit from Upstate Biotechnology Inc., according to the manufacturer's instructions. Briefly, cells were harvested when subconfluent and cell lysates were pre cleared with glutathione–agarose. GTP-bound Ras levels (1 mg of protein lysate) were determined by affinity precipitation (2 h at +4°C with gentle rocking) with immobilized (10 μl gel slurry) Raf-1 RBD (Ras binding domain). Raf-1 RBD-bound Ras levels were determined by immunoblot with an anti-pan-isoform-specific Ras monoclonal antibody (clone RAS10).

Real-time quantitative PCR

Total RNA was isolated by using the RNAeasy mini kit (Quiagen, Hilden, Germany) and was cleaned with RNase-free DNAse (Quiagen). Random-primed first strand cDNA was synthesized in a 50 μl reaction volume starting from 2 μg RNA by using the Gene Amp RNA PCR Core Kit (Applied Biosystems, Warrington, UK). The quantitative PCR reaction was performed by using the SYBR Green PCR Master mix (Applied Biosystems) in an iCycler apparatus (BioRad). Amplification reactions (25 μl final reaction volume) contained 200 nM of each primer, 3 mM $MgCl_2$ 300 μM dNTPs, 1x SYBR-Green PCR buffer, 0.1 U/μl A AmpliTaq Gold DNA Polymerase, 0.01 U/μl Amp Erase, RNase-free water and 2 μl cDNA samples. The thermal cycling conditions consisted of an initial cycle of 2 min at 50°C; a cycle of 10 min at 95°C and 40 cycles of 15 s of denaturation (95°C) followed by 1 min of annealing/extension (60°C). To verify the absence of non specific products, 80 cycles of melting (55°C for 10 s) were performed. In all cases, the melting curve confirmed that a single product was generated. Real-time amplification was monitored by measuring the increase in fluorescence caused by the SYBR-Green binding to double-stranded DNA. β actin amplification was used for normalization. Fluorescent threshold values were measured in triplicate and fold changes were calculated by the formula: $2^{-(\text{sample 1 } \Delta\text{Ct} - \text{sample 2 } \Delta\text{Ct})}$, where ΔCt is the difference between the amplification fluorescent thresholds of the mRNA of interest and the β actin mRNA. Primers were designed by using softwares available at the following web addresses: http://www-genome.wi.mit.edu/cgi-bin/primer/primer3_www.cgi; http://www.operon.com/oligos/toolkit.php? Primers sequences were as follows:

β actin forward: 5′-GTCAGGCAGCTCATAGCTCT-3′;
β actin reverse: 5′-TCGTGCGTGACATTAAAGAG-3′.
Bcl-2 forward: 5′-GATCCAGGATAACGGAGGCT-3′;
BcI-2 reverse: 5′-CTGAGCAGCGTCTTCAGAGA-3′;
Bax forward: 5′-CGAGCTGATCAGAACCATCA-3′;
Bax reverse: 5'-GGTCCCGAAGTAGGAGAGGA-3′.

Acknowledgments
We thank Francesca Carlomagno for her help with RET/PTC molecular constructs. We are grateful to Roberta Maestro for pBabe-Bcl-2 and to Jean Ann Gilder for editing the text. This study was supported by the Associazione Italiana per la Ricerca sul Cancro (AIRC), by the EC grant FIGH-CT1999-CHIPS, and by the Programma Biotecnologie legge 95/95 (MURST 5%). MDC was recipient of a fellowship of the BioGeM s.c.ar.l. (Biotecnologia e Genetica Molecolare nel Mezzogiorno d'Italia).

References

Borrello MG, Alberti L, Arighi E, Bongarzone I, Battistini C, Bardelli A, Pasini B, Piutti C, Rizzetti MG, Mondellini P, Radice MT and Pierotti MA. (1996). *Mol. Cell Biol.*, **16,** 2151–2163.

Cheng G and Meinkoth JL. (2001). *Oncogene*, **20,** 7334–7341

Corvi R, Martinez-Alfaro M, Harach HR, Zini M, Papotti M and Romeo G. (2001). *Lab. Invest.*, **81,** 1639–1645.

Downward J. (1998). *Curr. Opin. Genet. Dev.*, **8,** 49–54.

Dremier S, Taton M, Coulonval K, Nakamura T, Matsumoto K and Dumont JE. (1994). *Endocrinology*, **135,** 135–140.

Evan G and Littlewood T. (1998). *Science*, **281,** 1317–1322

Fusco A, Berlingieri MT, Di Fiore PP, Portella G, Grieco M and Vecchio G. (1987a). *Mol. Cell Biol.*, **7,** 3365–3370

Fusco A, Grieco M, Santoro M, Berlingieri MT, Pilotti S, Pierotti MA, Delia Porta G and Vecchio G. (1987b). *Nature*, **328,** 170–172

Gimm O. (2001). *Cancer Lett.*, **163,** 143–156

Grieco M, Santoro M, Berlingieri MT, Meliulo RM, Donghi R, Bongarzone I, Pierotti MA, Della Porta G, Fusco A and Vecchio G. (1990). *Cell*, **60,** 557–563

Jhiang SM. (2000). *Oncogene*, **19,** 5590–5597

Kauffmann-Zeh A, Rodriguez-Viciana P, Ulrich E, Gilbert C, Coffer P, Downward J and Evan G. (1997). *Nature*, **385,** 544–548

Kimura T, Van Keymeulen A, Goistein J, Fusco A, Dumont JE and Roger PP. (2001). *Endocr. Rev.*, **22,** 631–656

Lamy F, Wilkin F, Baptist M, Posada J, Roger PP and Dumont JE. (1993). *J. Biol. Chem.*, **268,** 8398–8401

Liu X, Vega QC, Decker RA, Pandey A, Worby CA and Dixon JE. (1996). *J. Biol. Chem.*, **271,** 5309–5312

Maestro R, Dei Tos AP, Hamamori Y, Krasnokutsky S, Sartorelli V, Kedes L, Doglioni C, Beach DH and Hannon GJ. (1999). *Genes Dev.*, **13,** 2207–2217

Manie S, Santoro M, Fusco A and Billaud M. (2001). *Trends Genet.*, **17,** 580–589

Melillo RM, Santoro M, Ong SH, Billaud M, Fusco A, Hadari YR, Schlessinger J and Lax I. (2001). *Mol. Cell Biol.*, **21,** 4177–4187

Mercalli E, Ghizzoni S, Arighi E, Alberti L, Sangregorio R, Radice MT, Gishizky ML, Pierotti MA and Borrello MG. (2001). *Oncogene*, **20,** 3475–3485

Monaco C, Visconti R, Barone MV, Pierantoni GM, Berlingieri MT, De Lorenzo C, Mineo A, Vecchio G, Fusco A and Santoro M. (2001). *Oncogene*, **20,** 599–608

Pierotti MA. (2001). *Cancer Lett.*, **166,** 1–7

Roger PP and Dumont JE. (1982). *FEBS Lett.*, **144,** 209–212

Santoro M, Dathan NA, Berlingieri MT, Bongarzone I, Paulin C, Grieco M, Pierotti MA, Vecchio G and Fusco A. (1994a). *Oncogene*, **9,** 509–516.

Santoro M, Melillo RM, Grieco M, Berlingieri MT, Vecchio G and Fusco A. (1993). *Cell Growth Differ.*, **4,** 77–84

Santoro M, Wong WT, Aroca P, Santos E, Matoskova B, Grieco M, Fusco A and di Fiore PP. (1994b). *Mol. Cell Biol.*, **14,** 663–675

Shirokawa JM, Elisei R, Knauf JA, Hara T, Wang J, Saavedra HI and Fagin JA. (2000). *Mol. Endocrinol.*, **14,** 1725–1738

Sugg SL, Ezzat S, Rosen IB, Freeman JL and Asa SL. (1998). *J. Clin. Endocrinol. Metab.*, **83,** 4116–4122

Tong Q, Xing S and Jhiang SM. (1997). *J. Biol. Chem.*, **272,** 9043–9047

Viglietto G, Chiappetta G, Martinez-TeHo FJ, Fukunaga FH, Tallini G, Rigopoulou D, Visconti R, Mastro A, Santoro M and Fusco A. (1995). *Oncogene*, **11,** 1207–1210

Xia Z, Dickens M, Raingeaud J, Davis RJ and Greenberg ME. (1995). *Science*, **270,** 1326–1331